JOURNAL OF OPTOELECTRONICS AND ADVANCED MATERIALS Vol. 25, No. 9-10, September – October 2023, p. 418 - 423

Reducing sidelobes in a Rugate filter to achieve high reflectivity

ELHAM JASIM MOHAMMAD*
Physics Science Department, College of Science, Mustansiriyah University, Baghdad, Iraq

In this paper, an optical interference Rugate filter was designed with high refractive index (2.4 with thickness= 57.292 nm), low refractive index (1.5 with thickness= 91.667 nm) and the reflectance spectra= 550 nm. Several optimized steps were performed to reduce the secondary sidelobes. The results show excellent flatness in the reflectance band. Apodization, quintic matching layers, and top AR coating are two effective means to eliminate the sidelobes near the stopband region. This paper goes into greater detail on analyzing data and explains what different statistical information can be calculated when designing optical filters, including mean, median, mode, and standard deviation.

(Received May 12, 2023; accepted October 6, 2023)

Keywords: Apodization, AR coating, Rugate filter, Refractive index, Reflectivity, Statistics analyzing data

1. Introduction

The “Rugate” word is derived from corrugated structures that are basis in nature and are selective reflects bands of specific wavelengths of light [1, 2]. Rugate filters are optical filters based on a dielectric coating, in which the refractive index is constantly changing, i.e. Rugate filter is classified as an optical filter and contains in its design an insulating reflecting mirror that has the property of selective reflection within a specified range of the light wavelength. This influence is completed through a periodical and continued alteration of the dielectric coating's refractive index [3].

Improving or controlling the spectral performance is an important use of optical interference films. These films represent a mixture of optical materials or very thin layers that differ by refractive index. When light passes and the difference in refractive index is available, then partial reflection occurs and the filter's optical spectrum determines the coherence of these reflections [2].

2. Design techniques of Rugate dielectric optical filters

The basic principle of Rugate filters is based on the dielectric coating, as there is a continuous change in the refractive index in some parts of the filter body. The name gradient index filters are used in order to distinguish between this filter and the conventional step index filters. The sinusoidal oscillation structure of the refractive index is the simplest example, which allows the phenomenon of reflection to occur in some narrow wavelength regions. In case of transmission, one gets a notch filter, which blocks some limited wavelength range, but in case of reflection, one gets a band-pass filter [2-7].

There are two techniques to study the reflection spectrum, theoretical analysis and numerical. When one study the theoretical analysis, conventional, by a step-index structure the gradient-index coating structure can be approximated with a larger number of steps index, and the change becomes very small, and depending on the analytical designs one can obtained a traditional filter curves.

While, using Fourier and inverse Fourier transform one can obtained many complex designs for filter curves [8].

For the low reflectivity's, one can choices the fact that, the reflection spectrum is related to the Fourier transforms of the spatial index profile. Also, the same method can use with high reflectivity's after made some modified to work perfectly [9-12].

The other way of Rugate filters is the numerical optimization techniques. In these techniques, one will optimize the details of the refractive index profile.

Now, it must be mentioned here, there are some cases about the refractive index profile, greater and maximum.

In the first case when the reflection is greater, the mirror wavelength determined using Bragg's theorem. While, in the second case, the series in the Bragg mirror sets alternating by: $n_L d_L + n_H d_H = \lambda_0/2$, where, λ_0 represent the wavelength, n_L and n_H represent the low and high refractive index respectively and the continuous change of the refractive index can be rewritten as [2]:

$$\int_0^d n(x)dx/d = \langle n \rangle d = \lambda_0/2$$

The integral solution is: $d = d_H + d_L$.

3. Results and discussions

In this study we used an ideal mixture material, where:

X range from= (300-1000) nm and Y range from= 1.4-2.4. Fused-Silica with thickness= 1mm used as a substrate, design wavelength= 550 nm, high refractive index= 2.4, low refractive index= 1.5 and design structure take the form:

HHHHLLHHLLHHLLHHLLHHLLHHLLHHLLHHLLHH

The reliability and accuracy of the data can be verified by calculating the standard deviation and differential data. Studying the statistics (mean, median, mode, and standard deviation) allowed one to view research in a different light and learn the importance of comparing data to one another, understanding statistics, and testing the significance of data. However, the methods used can help view data in large optical design scenarios. We used MATLAB and Open-Filters open source program. This paper goes into greater detail on analyzing data and explains what different statistical information can be calculated when designing optical filters.

3.1. Rugate filter

Fig. 1 shows the relations between the refractive index and penetration depth. Penetration depth can be defined as it represents the measure of the depth of any electromagnetic radiation or light that penetrates the material.

The refractive index-axis statistical analysis: mean= 1.963, median= 1.97, mode= 1.89 and the standard deviation= 0.25855. The max reached at 2.4.

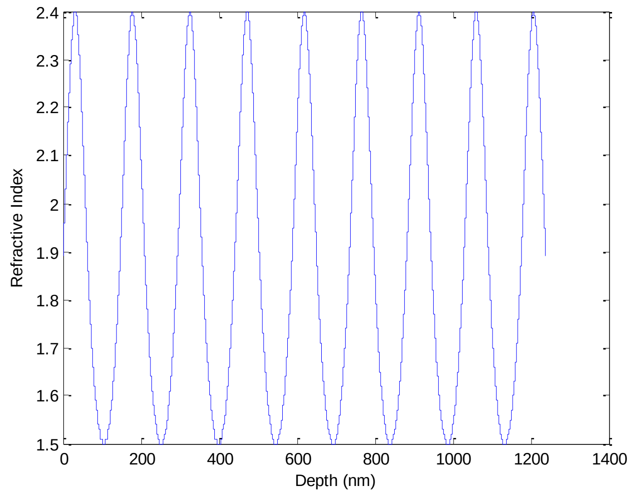

*Fig. **1**. Rugate filter refractive index fused silica substrate vs. depth without applying matching or apodization layers (color online)*

Fig. 2 shows the relation between the reflection phase (continues line) and transmission phase (dashed line) and wavelength, the resulting curve is without applying matching or apodization layers. The reflection phase-axis statistical analyses are: mean= 188, median= 186.8, mode= 79.71 and the standard deviation= 35.2. The reflection phase (continues line) max reached at 278.8 deg.

The transmission phase-axis statistical analyses are: mean= 190.9, median= 197.7, mode= 0.4177 and the standard deviation= 97.72. The transmission phase (dashed line) max reached at 360 deg.

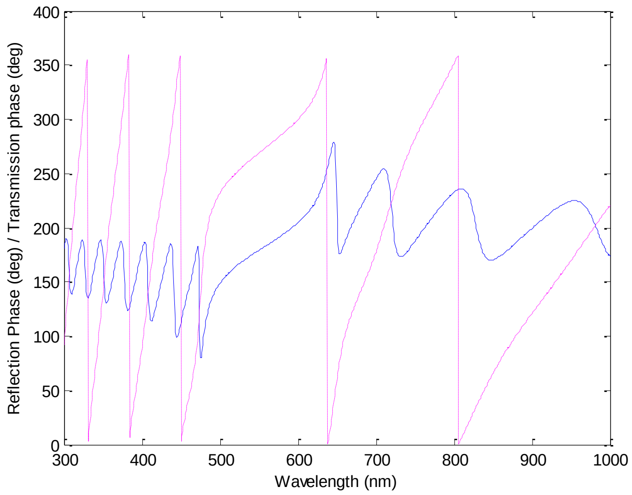

Fig. 2. Rugate filter reflection phase (continuous line)/ transmission phase (dashed line) vs. wavelength (color online)

Fig. 3 shows the relation between the reflection (continues line)/ transmission (dashed line) and wavelength. Note that, the secondary sidelobes are distributed on both sides of the near and far design wavelength region at 550 nm. The reflection-axis statistical analysis: mean= 0.3507, median= 0.212, mode= 0.9965 and the standard deviation= 0.3473, the reflection max reached at 0.997.

The transmission-axis statistical analysis: mean= 0.6493, median= 0.788, mode= 0.003035 and the standard deviation= 0.3473. The transmission max reached at 0.9887 and min reached at 0.003035.

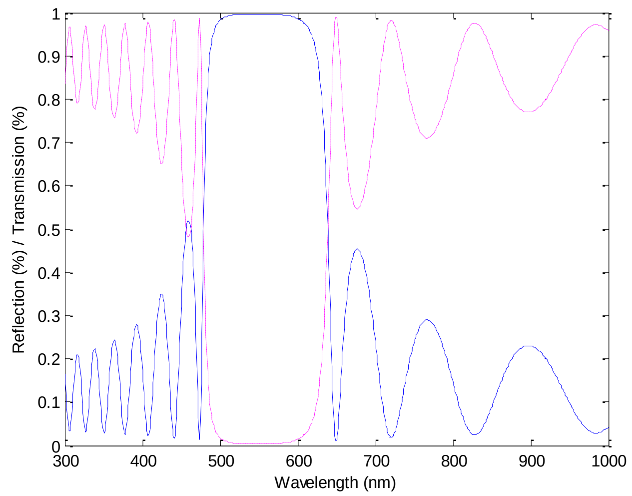

Fig. 3. Rugate filter reflection (continues line)/ transmission (dashed line) vs. the wavelength (color online)

3.2. Rugate filter with apodization

Apodization is one method that has proven effective in reducing ripples around reflection apertures, and it is applied to the profile of square wave and sine wave. Fig. 4 shows the relations between the refractive index and penetration depth.

The refractive index-axis statistical analysis: mean= 1.929, median= 1.92, mode= 1.89 and the standard deviation= 0.2131. The max reached at 2.4. Note, the curve contains several secondary sidelobes distributed on both sides of the near and far regions in depth = 600 nm, but this lobes have less pecks value than the curve before applying matching or apodization layers (Fig. 1).

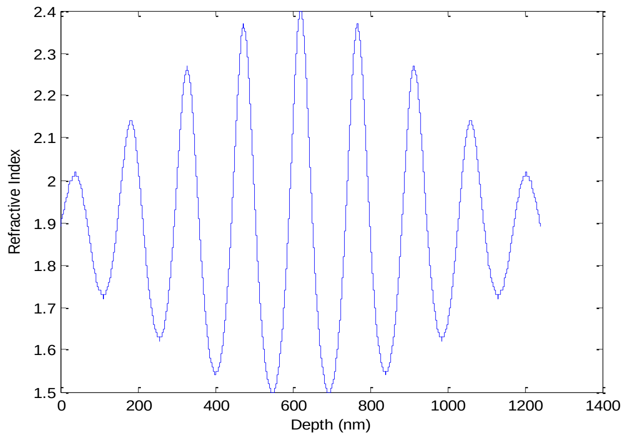

Fig. 4. Rugate filter with apodization refractive index on fused silica substrate vs. depth after applying apodization layers (color online)

Fig. 5 shows the relation between the reflection phase (continues line), transmission phase (dashed line) and wavelength. The reflection phase-axis statistical analysis: mean= 183.3, median= 181.9, mode= 4.016 and the standard deviation= 41.04.

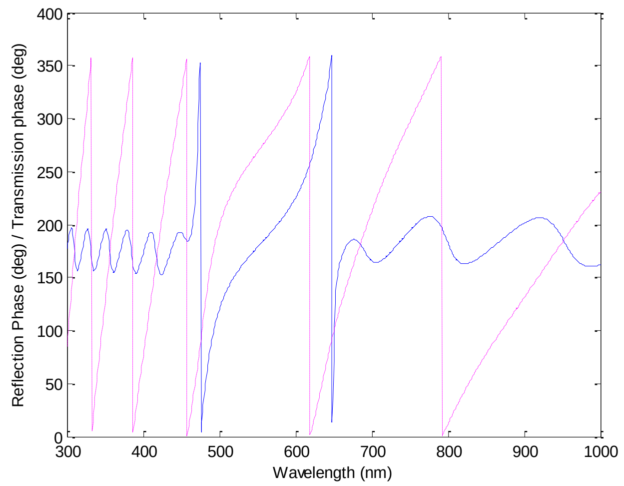

Fig. 5. Rugate filter with apodization reflection phase (continues line)/ transmission phase (dashed line) vs. wavelength (color online)

The reflection phase (continues line) max reached at 359.9 (deg). The transmission phase-axis statistical analysis: mean= 185.7, median= 191.2, mode= 0.04794 and the standard deviation= 98.31.

The transmission phase (dashed line) max reached at 358.9 (deg).

Fig. 6 shows the relation between the reflection (continues line)/ transmission (dashed line) and wavelength. The curve also have several secondary sidelobes distributed on either side of the near and far design wavelength region at 550 nm.

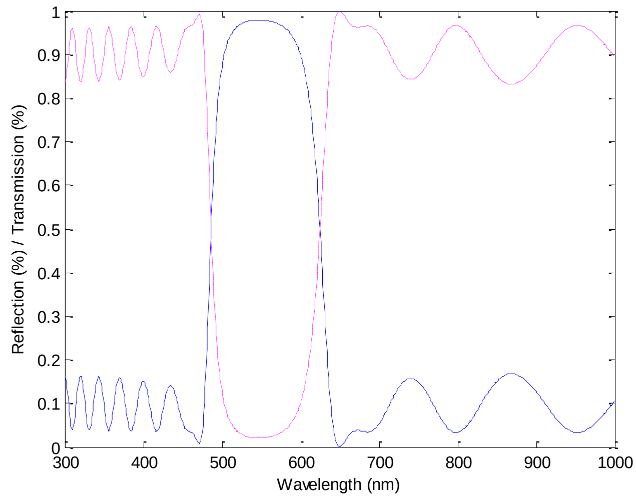

Fig. 6. Rugate filter with apodization reflection (continues line)/ transmission (dashed line) vs. wavelength (color online)

The reflection-axis statistical analysis: mean= 0.2536, median= 0.1107, mode= 0.04051 and the standard deviation= 0.3298. The reflection max reached at 0.9789 and it is less than the reflection max before applying matching or apodization layers (Fig. 3 the reflection max reached at 0.997).

The transmission-axis statistical analysis: mean= 0.7464, median= 0.8893, mode= 0.02111 and the standard deviation= 0.3298. The transmission max reached at 0.9989 and min reached at 0.02111 and it is greater than the transmission max value before applying matching or apodization layers (Fig. 3 the transmission max reached at 0.9887 and min reached at 0.003035).

3.3. Rugate filter with apodization and quintic matching layer

Fig. 7 shows the relation between the refractive index and penetration depth. The refractive index-axis statistical analysis: mean= 1.92, median= 1.91, mode= 1.89 and the standard deviation= 0.2148. The max reached at 2.4.

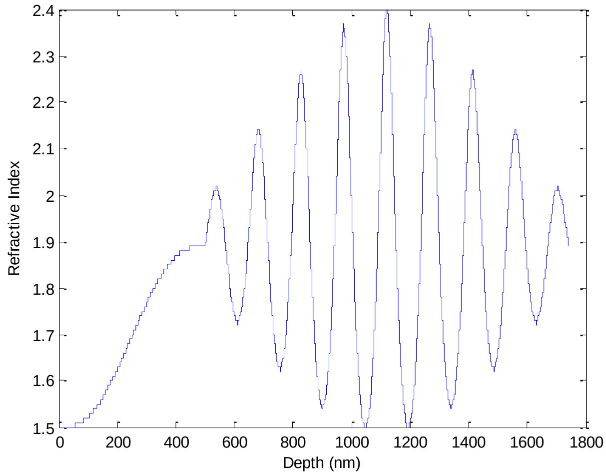

Fig. 7. Rugate filter with apodization and quintic matching layer refractive index vs. depth (color online)

The curve contains several secondary sidelobes distributed on both sides of the near and far regions of the depth at 1160 nm, but these lobes have less pecks value then the curve before applying apodization and quintic matching layer (Fig. 1).

Fig. 8 shows the relation between the reflection phases (continues line), transmission phase (dashed line) and wavelength with apodization and quintic matching layer.

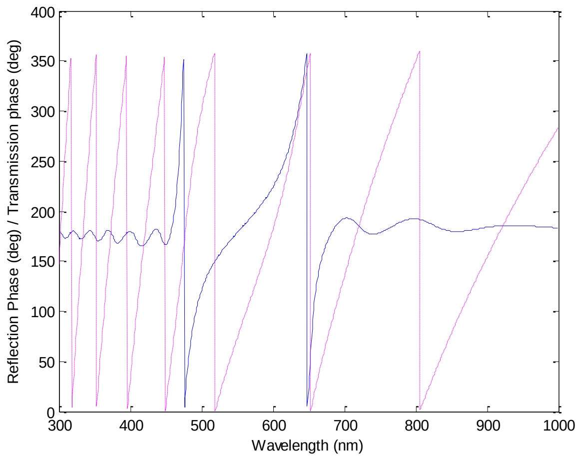

Fig. 8. Rugate filter with apodization and quintic matching layer reflection phase (continues line)/ transmission phase (dashed line) vs. wavelength (color online)

The reflection phase-axis statistical analysis: mean= 182.2, median= 181.8, mode= 3.516 and the standard deviation= 41.37. The reflection phase (continues line) max reached at 357.2 (deg). The transmission phase-axis statistical analysis: mean= 177.6, median= 179, mode= 0.1001 and the standard deviation= 99.35. The transmission phase (dashed line) max reached at 359.3 (deg).

Fig. 9 shows the relation between the reflection (continues line)/ Transmission (dashed line) and wavelength. Note, the curve having low sidelobes distributed on either side of the near and far regions of the design wavelength at 550 nm.

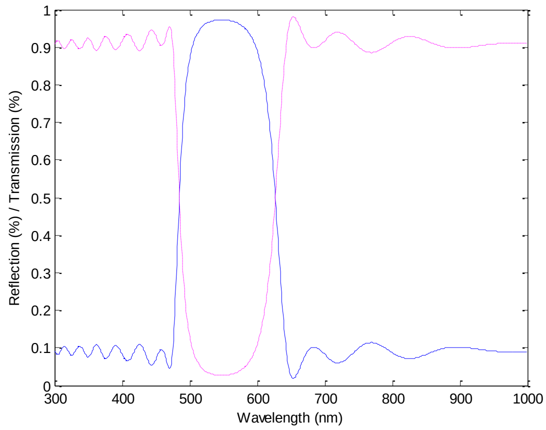

Fig. 9. Rugate filter with apodization and quintic matching layer reflection (continues line)/ transmission (dashed line) vs. wavelength (color online)

The reflection-axis statistical analysis: mean= 0.2561, median= 0.09516, mode= 0.07905 and the standard deviation= 0.3266. The reflection (continues line) max reached at 0.9733. The transmission-axis statistical analysis: mean= 0.7439, median= 0.9048, mode= 0.8916 and the standard deviation= 0.3266. The transmission (continues line) max reached at 0.9821 and min reached at 0.02673. In the figure below, the reflection value is about 97%, and it is also clear that there is a decrease in the number of sidelobes on both sides of the stop band. In spite of the reflection value we got near the stopping band, hard work must be intensified to reduce the value of the secondary sidelobes, which still have reflection values that affect the value of the fundamental peak.

3.4. Rugate filter with apodization, quintic matching layer, and top AR coating

Fig. 10 shows the relation between the refractive index and penetration depth.

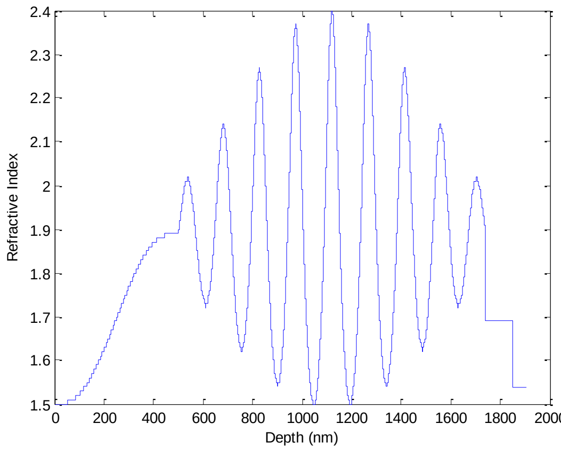

Fig. 10. Rugate filter with apodization, quintic matching layer, and top AR coating refractive index vs. depth (color online)

The refractive index-axis statistical analysis: mean= 1.92, median= 1.91, mode= 1.89 and the standard deviation= 0.215. The max reached at 2.4.

Fig. 11 shows the relation between the reflection phase (continues line), transmission phase (dashed line) and wavelength. The reflection phase-axis statistical analysis: mean= 175, median= 171.9, mode= 2.371 and the standard deviation= 49.36. The reflection phase (continues line) max reached at 357.7 (deg). The transmission phase-axis statistical analysis: mean= 177.7, median= 172.2, mode= 0.7192 and the standard deviation= 102.9. The transmission phase (dashed line) max reached at 359.6 (deg).

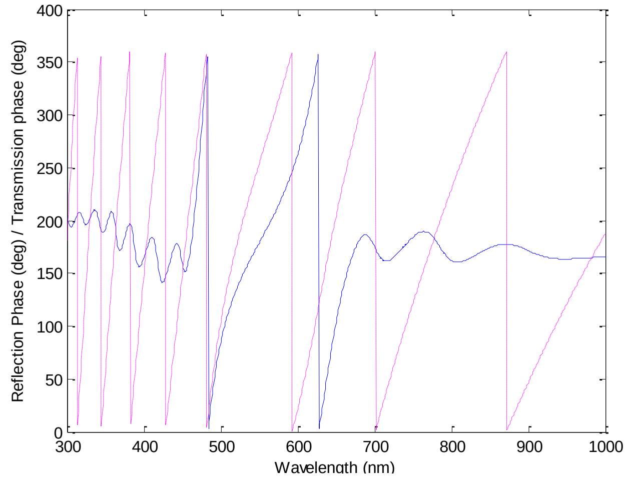

Fig. 11. Rugate filter with apodization, quintic matching layer, and top AR coating reflection phase (continues line)/ transmission phase (dashed line) vs. wavelength (color online)

Fig. 12 shows the relation between the reflection (continues line)/ Transmission (dashed line) and wavelength. Note, the curve having too low peaks ripple distributed on either side of the near and far regions of the design wavelength at 550 nm.

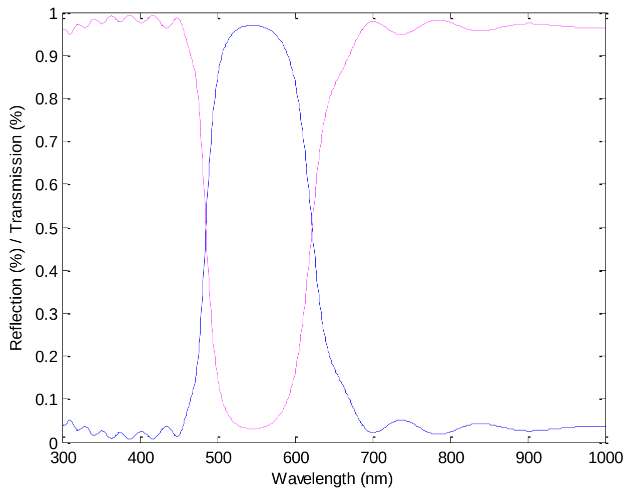

Fig. 12. Rugate filter with apodization, quintic matching layer, and top AR coating reflection (continues line)/ transmission (dashed line) vs. wavelength (color online)

The reflection-axis statistical analysis: mean= 0.2157, median= 0.03682, mode= 0.03651 and the standard deviation= 0.3362. The reflection (continues line) max reached at 0.9695. The transmission-axis statistical analysis: mean= 0.7843, median= 0.9632, mode= 0.03051 and the standard deviation= 0.3362. The transmission (continues line) max reached at 0.9931 and min reached at 0.03049. In the figure below, a slight decrease in reflection occurred and about 96% corresponding to a decrease in the value of the secondary peaks near and far on both sides of the stop band. Note, however, that the secondary peaks on either side of the stop band have decreased dramatically.

4. Conclusions

Linear interference with multiple refractive index oscillations occurs for the purpose of combining multiple reflection features. The lateral peaks of the reflection spectra of Rugate films can be significantly reduced by applying both the matching layers and apodization layers to the basic sinusoidal pattern and when applying apodization. When an appropriate number of sinusoidal repeats are combined the peak reflection is greatly modified.

The refractive index sinusoidal oscillation creates an isolated peak in the reflection spectrum, with no large side peaks.

The improved results significantly showed excellent suppression of the side peaks achieved around the stop range. The reflection peak achieved in the optimized design is about 97% and can be adjusted as per requirement.

Mixing the statistics (mean, median, mode, and standard deviation) and Rugate filter properties allowed one to view research in a different light and learn the importance of comparing data to one another, understanding statistics and testing the significance of data. However, the methods used can help view data in large optical designs scenarios.

References

[1] R. Paschotta, Rugate Filters, www.rp-photonics.com.
[2] H. A. Macleod, Thin-Film Optical Filters, Thin Film Center Inc. Tucson, Arizona, USA, p. 707, QC373.L5.M34 (2010), 4th Ed, Chap. 16.
[3] O. Stenzel, Optical Coatings: Material Aspects in Theory and Practice, Springer Series in Surface Sciences, 54, (2014).
[4] N. A. Vanyushkin, A. H. Gevorgyan, S. S. Golik, Optik **242**(3), 167343 (2021)
[5] H. A. Abu-Safia, A. I. Al-Sharif, I. O. Abu Aljarayesh, Applied Optics **32**(25), 4831 (1993).
[6] B. E. Perilloux, Thin-Film Design: Modulated Thickness and Other Stopband Design Methods. SPIE PRESS, International Society for Optical Engineering Bellingham, Washington USA, (2002).

[7] D. D. Luca, D. Kortge, E. D. Gennaro, R. Russo, P. Bermel, Optics Letters **47**(2), 230 (2022).
[8] E. V. Flores, R. M. Mejía, Applied Optics **62**(7), B7 (2023).
[9] P. G. Verly, J. A. Dobrowolski, W. J. Wild, R. L. Burton, Applied Optics **28**(14), 2864 (1989).
[10] B. G. Bovard, Applied Optics **32**(28), 5427 (1993).
[11] C. K. Carniglia, Applied Optics **28**(14), 2820 (1989).
[12] P. Baumeister, Applied Optics **25**(16), 2644 (1986).

*Corresponding author: elham.jasim@uomustansiriyah.edu.iq